

Carotid artery plaque composition and distribution: near-infrared spectroscopy and intravascular ultrasound analysis

Martin Horváth*, Petr Hájek, Cyril Štěchovský, Jakub Honěk, and Josef Veselka

Department of Cardiology, Charles University in Prague, 2nd Faculty of Medicine and Motol University Hospital, V Úvalu 84, 150 06 Prague 5, Czech Republic

KEYWORDS

Carotid artery plaque;
Plaque vulnerability;
Endothelial shear stress;
Near-infrared spectroscopy;
Intravascular ultrasound

Most atherosclerotic plaques (APs) form in typical predilection areas of low endothelial shear stress (ESS). On the contrary, previous data hinted that plaques rupture in their proximal parts where accelerated blood flow causes high ESS. It was postulated that high ESS plays an important role in the latter stages of AP formation and in its destabilization. Here, we used near-infrared spectroscopy (NIRS) to analyse the distribution of lipid core based on the presumed exposure to ESS. A total of 117 carotid arteries were evaluated using NIRS and intravascular ultrasound (IVUS) prior to carotid artery stenting. The point of minimal luminal area (MLA) was determined using IVUS. A stepwise analysis of the presence of lipid core was then performed using NIRS. The lipid core presence was quantified as the lipid core burden index (LCBI) within 2 mm wide segments both proximally and distally to the MLA. The analysed vessel was then divided into three 20 mm long thirds (proximal, middle, and distal) for further analysis. The maximal value of LCBI (231.9 ± 245.7) was noted in the segment localized just 2 mm proximally to MLA. The mean LCBI in the middle third was significantly higher than both the proximal (121.4 ± 185.6 vs. 47.0 ± 96.5 , $P < 0.01$) and distal regions (121.4 ± 185.6 vs. 32.4 ± 89.6 , $P < 0.01$). Lipid core was more common in the proximal region when compared with the distal region (mean LCBI 47.0 ± 96.5 vs. 32.4 ± 89.6 , $P < 0.01$).

Introduction

Atherosclerosis is a systemic disease that develops when endothelia are exposed to its common risk factors that are distributed uniformly throughout the blood stream.¹ It is also clear that despite this obvious and well-established fact, atherosclerotic plaques (APs) have a tendency to develop focally in specific predilection areas.¹ These typically include arterial bends and bifurcations.² This phenomenon is commonly explained by the direct hemodynamic effect of blood flow disturbances on endothelial cells, which can be expressed as the endothelial shear stress (ESS).² This is

defined as the frictional force exerted by the blood flow relative to the area of the endothelium.^{3,4}

Research in the past decades established ESS as an independent atherosclerotic risk factor.⁵

It is known that the exposure of endothelial cells to low ESS leads to a number of epigenetic modifications, which trigger changes that are important in the early stages of atherosclerosis.⁶⁻⁹ Conversely, high ESS has been linked to plaque destabilization in the latter stages of AP development.^{2,4,10} It is known that plaque ruptures occur more often in the areas of high ESS.¹¹ In vivo imaging previously revealed an association between high ESS and signs of plaque vulnerability.¹²⁻¹⁶ Recently, a study proved an association between the magnitude of ESS and the progression of coronary AP lipid content as detected by near-infrared spectroscopy (NIRS).¹⁷ We thus decided to perform a NIRS

*Corresponding author. Tel: +420 224434901, Fax: +420 224434920, Email: martin@horvath.cz

analysis of the lipid core distribution in carotid artery plaques based on the presumed exposure to ESS.

Material and methods

Study design and population

This is a single-centre study in patients that were enrolled to the previously published registry of patients that underwent NIRS-guided carotid artery stenting (CAS).^{18,19} The registry included consecutive patients that were scheduled for CAS due to either a symptomatic (more than 50% in a patient with a history of transient ischaemic attack or stroke in the previous 6 months) or asymptomatic (more than 70%) stenosis of the internal carotid artery (ICA) on non-invasive imaging. This was confirmed by invasive angiography prior to NIRS imaging in all cases. Every patient included in the study was ≥ 18 years old and had been considered eligible for CAS. Patients were excluded if they had renal insufficiency (estimated glomerular filtration rate ≤ 30 mL/min/1.73 m²), severe heart failure, active bleeding, intracranial bleeding, computed tomography, or angiographic evidence of intraluminal thrombus in the common carotid artery or ICA. Angiographic exclusion criteria were lesions with angiographic string sign or near-occlusion and where carotid anatomy was considered high risk for NIRS-intravascular ultrasound (IVUS) imaging (e.g. severe tortuosity of the common or ICA, Type III aortic arch).^{18,19} The study protocol was approved by Institutional Review Board and Ethical Committee (Motel University Hospital EK-755/14). All patients provided a written informed consent.

Procedure and image acquisition

All CAS procedures were performed in a single centre according to a protocol that was described previously.¹⁸⁻²⁵ The use of an embolic protection device with either distal protection [Emboshield NAV6 (Abbott Vascular, Redwood City, CA, USA)], or proximal protection [Mo.Ma (Invatec, Roncadelle, Italy)] was mandatory prior to the NIRS imaging. The choice of the protection device was based on the decision of an experienced operator. The intravascular imaging was performed after the initial angiography with the 3.2 F TVC-Catheter (Infraredx Burlington, MA, USA) which combines both NIRS and IVUS. All NIRS-IVUS images were obtained prior to CAS. The catheter was advanced over 0014" guidewire 30 mm distal to the lesion and start position was recorded with fluoroscopy and contrast injection. A 60 mm long automated pullback at the speed of 0.5 mm/s was then performed.

Definitions and data analysis

All NIRS-IVUS data acquired during the imaging procedure were stored in the Digital Imaging and Communications in Medicine (DICOM) format for a subsequent off-line analysis using the dedicated QIVUS post-processing software (Medis, Leiden, the Netherlands). A semi-automatic analysis of the greyscale IVUS data was performed using this software. In each patient, the contours of the lumen and external elastic membrane (EEM) were identified. This allowed us to perform the basic IVUS measurements, which included the

plaque burden, vessel area, and luminal area. Minimal luminal area (MLA) was defined as the IVUS frame in which the area of the lumen was the smallest.

The results of NIRS were presented simultaneously with the IVUS data as a colour-coded probability map of lipid presence, which is called NIRS chemogram. The map depicts the probability of lipid presence based on NIRS data on a scale from dark red to light yellow for the NIRS-derived lipid core plaque (LCP) (probability of lipid presence exceeding 0.6). The amount of lipids is quantified as the lipid core burden index (LCBI), which is a unitless measure defined as the fraction of yellow pixels on the chemogram multiplied by 1000.^{18,23,26,27}

During the actual analysis, we first identified the site of the MLA. This acted as a reference point from which a step-wise analysis of the NIRS data was performed in both directions. The LCBI was determined within 2 mm wide segments. The analysed vessel was then divided into three 20 mm long thirds (proximal, middle, and distal) for further analysis. The reason for that was that the proximal and middle parts of the plaque are exposed to higher ESS.^{28,29} No quantification of the ESS was performed in the study.

Statistical analysis

Continuous variables are presented as mean \pm standard deviation, and discrete data are presented as absolute numbers (%). Student's *t*-test was used as appropriate for the comparison between the regions. Statistical significance was set at the two-tailed 0.05 level. GraphPad prism 6 (GraphPad Software, La Jolla, CA, USA) was used for the computations.

Results

Baseline characteristics

A total of 117 patients were enrolled in our study (67.1 ± 8.3 years, 68% men). There was a high prevalence of the conventional atherosclerotic risk factors (Table 1). Eighteen of these patients (15.4%) had a symptomatic

Table 1 Here, we provide the baseline characteristics of our study population

Number of patients, <i>N</i>	117
Males, <i>n/N</i> (%)	78/117 (68)
Age (years), mean \pm SD	67.1 \pm 8.3
BMI (kg/m ²), mean \pm SD	28.1 \pm 4.1
Symptomatic stenoses, <i>n/N</i> (%)	18/117 (15)
Arterial hypertension, <i>n/N</i> (%)	103/117 (88)
Ischaemic heart disease, <i>n/N</i> (%)	56/117 (43)
Smoking, <i>n/N</i> (%)	43/117 (37)
Diabetes mellitus, <i>n/N</i> (%)	40/117 (34)
Hs-CRP (mg/L), mean \pm SD	2.89 \pm 2.29
Creatinin (μ mol/L), mean \pm SD	85.5 \pm 26.0
Total cholesterol (mmol/L), mean \pm SD	4.36 \pm 0.93
LDL cholesterol (mmol/L), mean \pm SD	2.47 \pm 0.85

CRP, C-reactive protein; LDL, low-density lipoprotein; *n*, number of patients; *N*, total number of patients enrolled; SD, standard deviation.

stenosis, all other patients were asymptomatic (84.6%). Distal embolic protection device was used in 104 (88.9%) of the patients, while proximal embolic protection was used in 23 (20.5%) patients. A combination of both devices was utilized in 11 patients (9.4%). One (0.9%) peri-procedural transient ischaemic attack occurred during the stenting procedure. Baseline characteristics of the study population are summarized in *Table 1*.

Near-infrared spectroscopy and intravascular ultrasound analysis

The area of MLA was detectable in all patients. Near-infrared spectroscopy chemograms were evaluable in all 117 cases. The highest mean value of LCBI (231.9 ± 245.7) was noted in the segment localized just 2 mm proximally to MLA (see *Figures 1A* and *2*). The mean LCBI in the middle

third was significantly higher than both the proximal (mean LCBI 121.4 ± 185.6 vs. 47.0 ± 96.5 , $P < 0.01$) and distal regions (mean LCBI 121.4 ± 185.6 vs. 32.4 ± 89.6 , $P < 0.01$). Near-infrared spectroscopy-derived LCP was more common in the proximal region when compared with the distal region (mean LCBI 47.0 ± 96.5 vs. 32.4 ± 89.6 , $P < 0.01$). These results are summarized in *Figure 1B-D*.

Discussion

The principle findings of the study may be summarized as follows: (i) lipids were most often detectable around the maximum of the carotid stenosis and (ii) the NIRS-derived LCP was detected more commonly in the proximal parts of the carotid AP when compared with the distal tertile.

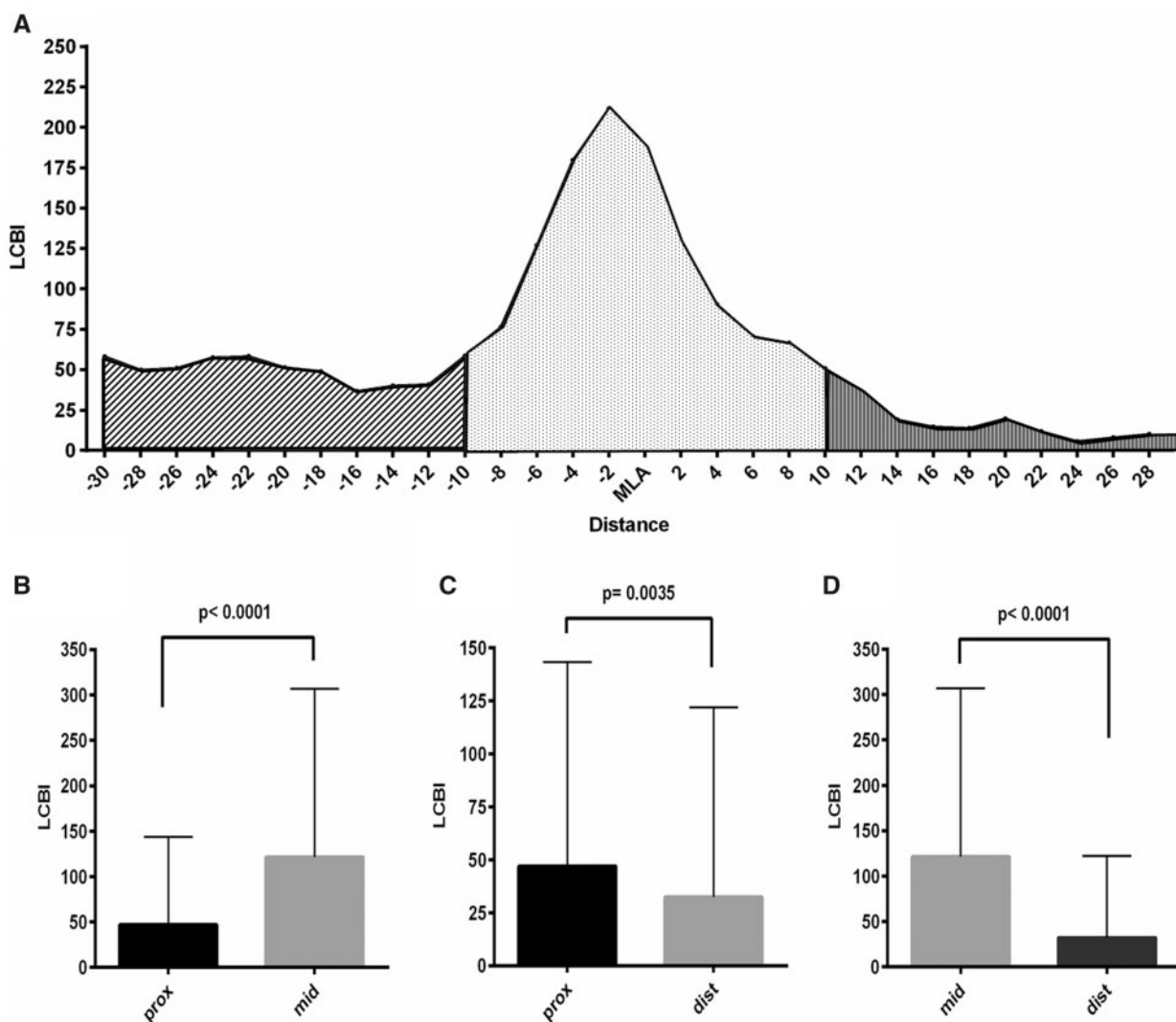


Figure 1 The maximal value of lipid core burden index (231.9 ± 245.7) was noted in the segment localized just 2 mm proximally to minimal luminal area (A). The mean lipid core burden index in the middle third was significantly higher (mean lipid core burden index 121.4 ± 185.6 vs. 46.97 ± 96.52 , $P < 0.01$) when compared with the proximal tertile (B). Similarly, when comparing lipid core burden index in the distal and middle thirds (mean lipid core burden index 32.44 ± 89.61 vs. 121.4 ± 185.6 , $P < 0.01$), we found a statistically significant difference (D). (C) The statistically significant difference between near-infrared spectroscopy-derived lipid core plaque in the proximal region when compared with the distal one (mean lipid core burden index 46.97 ± 96.52 vs. 32.44 ± 89.61 , $P < 0.01$).

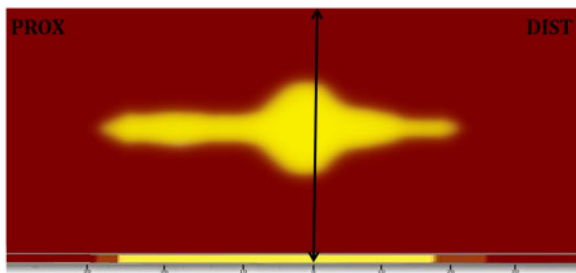


Figure 2 To better illustrate our results, we provide the reader with an artificially created chemogram, which depicts the mean lipid core burden index in individual arterial segments. The chemogram is the basic output of near-infrared spectroscopy. Yellow colour indicates the presence and location of lipids in the lesion. The x-axis represents the distance of the pullback within the artery, whereas the y-axis signifies rotation of the imaging probe from 0° to 360°.

These observations may potentially be explained by the influence of ESS. Research in the past decades established ESS as an independent atherosclerotic risk factor.⁵ It is known that the exposure of endothelial cells to low ESS leads to a number of epigenetic modifications, which trigger changes in their physiology due to altered protein expression.⁶⁻⁹ Endothelia that are exposed to ESS disturbance in animal models tend to express different surface molecules, which leads to modifications in their shape, permeability, the ability to bind different molecules such as low-density lipoprotein particles and the expression of inflammatory cell receptors.^{2,6,30-33} This translates into lipid deposition, increase in oxidative stress and activation of inflammatory pathways.^{6,12} All of these undesirable changes are important in the early stages of AP development.²

High ESS has been linked to plaque destabilization in the latter stages of AP development.^{2,4,10} Although the pathophysiology behind this phenomenon is not yet fully understood, we have quite a lot of insight from both basic science and clinical research.^{11-17,33-38} An increase in nitric oxide synthase expression has been described in an animal carotid artery cross-clamp model of high ESS.³⁴⁻³⁷ One of its consequences is over-expression of matrix metalloproteinases.³⁴⁻³⁷ Moreover, high ESS causes overexpression of plasmin and transforming growth factor beta.³⁸ These changes lead to undesirable alterations to the composition of extracellular matrix and ultimately to its gradual degradation.³⁸ Another outcome of nitric oxide over-production is the macrophage mediated apoptosis of smooth-muscle cells.³⁸ This participates on the formation of necrotic core within AP and changes that may ultimately lead to its rupture.³⁸ Indeed, it has been observed that atherosclerotic plaque ruptures occur most frequently in the areas of high ESS.^{11,13} *In vivo* imaging studies with IVUS and optical coherence tomography found the presence of various signs of vulnerability in the proximal parts of coronary plaques.^{12,30} When paired with three-dimensional arterial reconstruction and ESS assessment by computational fluid dynamics the imaging proved that signs of vulnerability are more often found in the high ESS regions.¹²⁻¹⁶ Recently, a similar finding has also been described in a prospective study using the NIRS-IVUS catheter in the coronary arteries.¹⁷ Here the

authors found an association between the magnitude of baseline ESS and the progression of LCBI leading to the development of lipid-rich plaque at follow-up.¹⁷ We hypothesize, based on these findings, that our observations can be explained by the distribution of ESS in the carotid AP.³⁹⁻⁴¹

To our knowledge, this study is the first to investigate the spatial distribution of NIRS-derived LCP in the carotid arteries. Near-infrared spectroscopy is a technique that has been intentionally developed for the identification of lipid cores within AP through determination of their chemical composition based on the different absorbance of the near-infrared spectra.^{42,43} This presumably makes it an optimal tool for the evaluation of plaque vulnerability. Most of the previously published NIRS research focused on the coronary arteries, where the catheter has been validated against autopsy specimens.^{26,44} It was proven that high NIRS-derived LCBI predicts lesions that cause acute coronary syndromes.⁴⁵⁻⁴⁸ Different reports found an association between baseline LCBI and future coronary events.^{46,49-52} In light of these findings and the abovementioned association between the magnitude of ESS and local progression of LCBI we believe that the observation of NIRS-derived LCPs in the proximal parts of AP might be translatable into clinical events. A less invasive estimation of ESS might possibly help with the choice between optimal medical therapy and invasive treatment. The information about the localization of lipid core might help with the fine-tuning of CAS procedures in order to cover the whole lesion and to prevent distal embolization in a manner that was described in the coronary arteries.^{53,54} However, these are only hypotheses that are currently not supported by any scientific evidence. No prospective study using NIRS imaging has been published in the carotid artery research to date.

Our team previously documented the safety and feasibility of NIRS imaging in the carotid arteries.²¹ We documented that LCBI decreases during CAS, which might be attributable to the distal embolization of LCPs as was documented in a case report.^{19,55} This leads us to believe that NIRS can truly detect LCPs in the carotid arteries despite their larger diameter when compared with coronary arteries. However, the absence of a validation of the NIRS catheter for larger vessels is an important limitation to consider when interpreting our results. A possible explanation for the high detection of lipids around the maximum of stenoses may solely be its better detection due to a smaller distance between the probe and the vessel wall. Nevertheless, this alone would not explain the fact that LCPs were more often detected in the proximal parts where the average arterial caliber is largest.

This study has several limitations. The most obvious one is the lack of ESS quantification. We assessed our data retrospectively from the previously mentioned registry, which means that we were not able to obtain the data needed for computational fluid dynamics reconstruction. The potential association between our observation and ESS thus remains to be further tested. Other limitations include the observational design and the relatively small study sample. This did not allow us to reliably verify whether the observations translate into any clinically relevant outcomes. The study should therefore be viewed as a pilot project aiming to generate hypotheses for further research.

Conclusion

In patients with significant carotid artery disease, lipid core is more frequent in areas located proximally to the maximum of stenosis.

Funding

Research supported by MH CZ-DRO, University Hospital Motol, Prague, Czech Republic; 00064203; SVV-2013-266509 from the Charles University in Prague. This paper was published as part of a supplement financially supported by the Cardiovascular Research Program of the Charles University 'Progres Q38'.

Conflict of interest: none declared.

References

- Kwak BR, Bäck M, Bochaton-Piallat M-L, Caligiuri G, Daemen M, Davies PF, Hofer IE, Holvoet P, Jo H, Krams R, Lehoux S, Monaco C, Steffens S, Virmani R, Weber C, Wentzel JJ, Evans PC. Biomechanical factors in atherosclerosis: mechanisms and clinical implications. *Eur Heart J* 2014;**35**:3013-3020, 3020a-3020d.
- Hung OY, Brown AJ, Ahn SG, Veneziani A, Giddens DP, Samady H. Association of wall shear stress with coronary plaque progression and transformation. *Interv Cardiol Clin* 2015;**4**:491-502.
- Fernandes DC, Araujo TLS, Tanaka LY. Hemodynamic forces in the endothelium: from mechanotransduction to implications on development of atherosclerosis. *Endothel Cardiovasc Dis* 2018;**85**:95.
- Makris GC, Nicolaides AN, Xu XY, Geroulakos G. Introduction to the biomechanics of carotid plaque pathogenesis and rupture: review of the clinical evidence. *Br J Radiol* 2010;**83**:729-735.
- Cunningham KS, Gottlieb AI. The role of shear stress in the pathogenesis of atherosclerosis. *Lab Invest* 2005;**85**:9-23.
- Stone PH, Coskun AU, Kintlay S, Popma JJ, Sonka M, Wahle A, Yeghiazarians Y, Maynard C, Kuntz RE, Feldman CL. Regions of low endothelial shear stress are the sites where coronary plaque progresses and vascular remodelling occurs in humans: an in vivo serial study. *Eur Heart J* 2007;**28**:705-710.
- K Van der H, Hierck BP, Krams R, R de C, Cheng C, Baiker M, Pourquie M, Alkemade FE, DeRuiter MC, Gittenberger-de Groot AC, Poelmann RE. Endothelial primary cilia in areas of disturbed flow are at the base of atherosclerosis. *Atherosclerosis* 2008;**196**:542-550.
- Lee D-Y, Chiu J-J. Atherosclerosis and flow: roles of epigenetic modulation in vascular endothelium. *J Biomed Sci* 2019;**26**:56.
- Dunn J, Simmons R, Thabet S, Jo H. The role of epigenetics in the endothelial cell shear stress response and atherosclerosis. *Int J Biochem Cell Biol* 2015;**67**:167-176.
- Cheng C, Tempel D, Haperen R, van Baan AVD, Grosveld F, Daemen M, Krams R, Crom RD. Atherosclerotic lesion size and vulnerability are determined by patterns of fluid shear stress. *Circulation* 2006;**113**:2744-2753.
- Groen HC, Gijssen FJH, Lugt AVD, Ferguson MS, Hatsukami TS, Steen AVD, Yuan C, Wentzel JJ. Plaque rupture in the carotid artery is localized at the high shear stress region: a case report. *Stroke* 2007;**38**:2379-2381.
- Wentzel JJ, Schuurbiens JCH, Gonzalo Lopez N, Gijssen FJH, Giessen AVD, Groen HC, Dijkstra J, Garcia-Garcia HM, Serruys PW. In vivo assessment of the relationship between shear stress and necrotic core in early and advanced coronary artery disease. *EuroIntervention* 2013;**9**:989-995.
- Costopoulos C, Huang Y, Brown AJ, Calvert PA, Hoole SP, West NEJ, Gillard JH, Teng Z, Bennett MR. Plaque rupture in coronary atherosclerosis is associated with increased plaque structural stress. *JACC Cardiovasc Imaging* 2017;**10**:1472-1483.
- Eshtehardi P, McDaniel MC, Suo J, Dhawan SS, Timmins LH, Binongo JNG, Golub LJ, Corban MT, Finn AV, Oshinsk JN, Quyyumi AA, Giddens DP, Samady H. Association of coronary wall shear stress with atherosclerotic plaque burden, composition, and distribution in patients with coronary artery disease. *J Am Heart Assoc* 2012;**1**:e002543.
- Samady H, Eshtehardi P, McDaniel MC, Suo J, Dhawan SS, Maynard C, Timmins LH, Quyyumi AA, Giddens DP. Coronary artery wall shear stress is associated with progression and transformation of atherosclerotic plaque and arterial remodeling in patients with coronary artery disease. *Circulation* 2011;**124**:779-788.
- Yamamoto E, Thondapu V, Poon E, Sugiyama T, Fracassi F, Dijkstra J, Lee H, Ooi A, Bartis P, Jang I-K. Endothelial shear stress and plaque erosion. *JACC Cardiovasc Imaging* 2019;**12**:374-375.
- Shishikura D, Sidharta SL, Honda S, Takata K, Kim SW, Andrews J, Montarello N, Delacroix S, Baillie T, Worthley MI, Psaltis PJ, Nicholls SJ. The relationship between segmental wall shear stress and lipid core plaque derived from near-infrared spectroscopy. *Atherosclerosis* 2018;**275**:68-73.
- Štěchovský C, Hájek P, Horváth M, Špaček M, Veselka J. Near-infrared spectroscopy combined with intravascular ultrasound in carotid arteries. *Int J Cardiovasc Imaging* 2016;**32**:181-188.
- Štěchovský C, Hájek P, Horváth M, Veselka J. Effect of stenting on the near-infrared spectroscopy-derived lipid core burden index of carotid artery plaque. *EuroIntervention* 2019;**15**:e289-e296.
- Veselka J, Špaček M, Hájek P, Horváth M, Štěchovský C, Zimolová P. Impact of single versus double vessel carotid disease on long-term survival in patients treated with carotid stenting. *Int J Cardiol* 2014;**176**:1299-1300.
- Štěchovský C, Hájek P, Horváth M, Špaček M, Veselka J. Composition of carotid artery stenosis and restenosis: a series of patients assessed with intravascular ultrasound and near-infrared spectroscopy. *Int J Cardiol* 2016;**207**:64-66.
- Spacek M, Stechovsky C, Horvath M, Hajek P, Zimolova P, Veselka J. Evaluation of cerebrovascular reserve in patients undergoing carotid artery stenting and its usefulness in predicting significant hemodynamic changes during temporary carotid occlusion. *Physiol Res* 2016;**65**:71-79.
- Horváth M, Hájek P, Štěchovský C, Honěk J, Veselka J. Intravascular near-infrared spectroscopy: a possible tool for optimizing the management of carotid artery disease. *Int J Angiol* 2015;**24**:198-204.
- Veselka J, Černá D, Zimolová P, Martinkovičová L, Fiedler J, Hájek P, Malý M, Zemánek D, Duchonová R. Feasibility, safety, and early outcomes of direct carotid artery stent implantation with use of the FilterWire EZ™ Embolic Protection System. *Catheter Cardiovasc Interv* 2009;**73**:733-738.
- Veselka J, Černá D, Zimolová P, Blasko P, Fiedler J, Hájek P, Malý M, Zemánek D, Duchonová R. Thirty-day outcomes of direct carotid artery stenting with cerebral protection in high-risk patients. *Circ J* 2007;**71**:1468-1472.
- Gardner CM, Tan H, Hull EL, Lisauskas JB, Sum ST, Meese TM, Jiang C, Madden SP, Caplan JD, Burke AP, Virmani R, Goldstein J, Muller JE. Detection of lipid core coronary plaques in autopsy specimens with a novel catheter-based near-infrared spectroscopy system. *JACC Cardiovasc Imaging* 2008;**1**:638-648.
- Horvath M, Hajek P, Stechovsky C, Honek J, Spacek M, Veselka J. The role of near-infrared spectroscopy in the detection of vulnerable atherosclerotic plaques. *Arch Med Sci* 2016;**12**:1308-1316.
- Wang Y, Qiu J, Luo S, Xie X, Zheng Y, Zhang K, Ye Z, Liu W, Gregersen H, Wang G. High shear stress induces atherosclerotic vulnerable plaque formation through angiogenesis. *Regen Biomater* 2016;**3**:257-267.
- Cho YI, Cho DJ, Rosenson RS. Endothelial shear stress and blood viscosity in peripheral arterial disease. *Curr Atheroscler Rep* 2014;**16**:404.
- Shyy J-J, Chien S. Role of integrins in endothelial mechanosensing of shear stress. *Circ Res* 2002;**91**:769-775.
- Aquila G, Morelli MB, Vieceli Dalla Sega F, Fortini F, Nigro P, Caliceti C, Ferracin M, Negrini M, Pannuti A, Bonora M, Pinton P, Ferrari R, Rizzo P. Heart rate reduction with ivabradine in the early phase of atherosclerosis is protective in the endothelium of ApoE-deficient mice. *J Physiol Pharmacol* 2018;**69**:35-52.
- Xing R, Moerman AM, Ridwan RY, Gaalen KV, Meester EJ, Steen AVD, Evans PC, Gijssen FJH, Heiden KVD. The effect of the heart rate lowering drug Ivabradine on hemodynamics in atherosclerotic mice. *Sci Rep* 2018;**8**:14014.

33. Le L, Duckles H, Schenkel T, Mahmoud M, Tremoleda J, Wylezinska-Arridge M, Ali M, Bowden N, Villa-Uriol M-C, Heiden KVD, Xing R, Gijssen F, Wentzel J, Lawrie A, Feng S, Arnold N, Gsell W, Lungu A, Hose R, Spencer T, Halliday I, Ridger V, Evans P. Heart rate reduction with ivabradine promotes shear stress-dependent anti-inflammatory mechanisms in arteries. *Thromb Haemost* 2016;116:181-190.
34. Cheng C, Haperen R, van Waard MD, Damme LV, Tempel D, Hanemaaijer L, Cappellen GV, Bos J, Slager CJ, Duncker DJ, Steen AVD, Crom RD, Krams R. Shear stress affects the intracellular distribution of eNOS: direct demonstration by a novel *in vivo* technique. *Blood* 2005;106:3691-3698.
35. Wang H-H, Hsieh H-L, Yang C-M. Nitric oxide production by endothelin-1 enhances astrocytic migration via the tyrosine nitration of matrix metalloproteinase-9. *J Cell Physiol* 2011;226:2244-2256.
36. Dumont O, Loufrani L, Henrion D. Key role of the NO-pathway and matrix metalloproteinase-9 in high blood flow-induced remodeling of rat resistance arteries. *Arterioscler Thromb Vasc Biol* 2007;27:317-324.
37. Death AK, Nakhla S, McGrath KCY, Martell S, Yue DK, Jessup W, Celermajer DS. Nitroglycerin upregulates matrix metalloproteinase expression by human macrophages. *J Am Coll Cardiol* 2002;39:1943-1950.
38. Slager C, Wentzel J, Gijssen F, Thury A, Wal AVD, Schaar J, Serruys P. The role of shear stress in the destabilization of vulnerable plaques and related therapeutic implications. *Nat Clin Pract Cardiovasc Med* 2005;2:456-464.
39. Davies PF. Hemodynamic shear stress and the endothelium in cardiovascular pathophysiology. *Nat Clin Pract Cardiovasc Med* 2009;6:16-26.
40. Kundu PK, Cohen IM, Dowling DR, Tryggvason G. Fluid mechanics-6th Edition. [online] Elsevier.com. Available at: <<https://www.elsevier.com/books/fluid-mechanics/kundu/978-0-12-405935-1>>
41. Cebral JR, Castro MA, Putman CM, Alperin N. Flow-area relationship in internal carotid and vertebral arteries. *Physiol Meas* 2008;29:585-594.
42. Horváth M, Hájek P, Štečhořský C, Veselka J. Vulnerable plaque imaging and acute coronary syndrome. *Cor Vasa* 2014;56:e362-e368.
43. Moreno PR, Lodder RA, Purushothaman KR, Charash WE, O'Connor WN, Muller JE. Detection of lipid pool, thin fibrous cap, and inflammatory cells in human aortic atherosclerotic plaques by near-infrared spectroscopy. *Circulation* 2002;105:923-927.
44. Waxman S, Dixon SR, L'Allier P, Moses JW, Petersen JL, Cutlip D, Tardif J-C, Nesto RW, Muller JE, Hendricks MJ, Sum ST, Gardner CM, Goldstein JA, Stone GW, Krucoff MW. *In vivo* validation of a catheter-based near-infrared spectroscopy system for detection of lipid core coronary plaques: initial results of the SPECTACL study. *JACC Cardiovasc Imaging* 2009;2:858-868.
45. Madder RD, Husaini M, Davis AT, Oosterhout SV, Harnek J, Göteborg M, Erlinge D. Detection by near-infrared spectroscopy of large lipid cores at culprit sites in patients with non-st-segment elevation myocardial infarction and unstable angina. *Catheter Cardiovasc Interv* 2015;86:1014-1021.
46. Karlsson S, Anesäter E, Fransson K, Andell P, Persson J, Erlinge D. Intracoronary near-infrared spectroscopy and the risk of future cardiovascular events. *Open Heart* 2019;6:e000917.
47. Madder RD, Goldstein JA, Madden SP, Puri R, Wolski K, Hendricks M, Sum ST, Kini A, Sharma S, Rizik D, Brilakis ES, Shunk KA, Petersen J, Weisz G, Virmani R, Nicholls SJ, Maehara A, Mintz GS, Stone GW, Muller JE. Detection by near-infrared spectroscopy of large lipid core plaques at culprit sites in patients with acute ST-segment elevation myocardial infarction. *JACC Cardiovasc Interv* 2013;6:838-846.
48. Madder RD, Puri R, Muller JE, Harnek J, Göteborg M, VanOosterhout S, Chi M, Wohns D, McNamara R, Wolski K, Madden S, Sidharta S, Andrews J, Nicholls SJ, Erlinge D. Confirmation of the intracoronary near-infrared spectroscopy threshold of lipid-rich plaques that underlie st-segment-elevation myocardial infarction. *Arterioscler Thromb Vasc Biol* 2016;36:1010-1015.
49. Daneke BA, Karatasakis A, Karacsonyi J, Alame A, Resendes E, Kalsaria P, Nguyen-Trong P-K, Rangan BV, Roesle M, Abdullah S, Banerjee S, Brilakis ES. Long-term follow-up after near-infrared spectroscopy coronary imaging: insights from the lipid cORe plaque association with Clinical events (ORACLE-NIRS) registry. *Cardiovasc Revasc Med* 2017;18:177-181.
50. Schuurman A-S, Vroegindewey M, Kardys I, Oemrawsingh RM, Cheng JM, Boer SD, Garcia-Garcia HM, Geuns R-JV, Regar ES, Daemen J, Miegheem NM, van Serruys PW, Boersma E, Akkerhuis KM. Near-infrared spectroscopy-derived lipid core burden index predicts adverse cardiovascular outcome in patients with coronary artery disease during long-term follow-up. *Eur Heart J* 2018;39:295-302.
51. Waksman R, Di Mario C, Torguson R, Ali ZA, Singh V, Skinner WH, Artis AK, Cate TT, Powers E, Kim C, Regar E, Wong SC, Lewis S, Wykrzykowska J, Dube S, Kazziha S, van der Ent M, Shah P, Craig PE, Zou Q, Kolm P, Brewer HB, Garcia-Garcia HM, Samady H, Tobis J, Zainea M, Leimbach W, Lee D, Lalonde T, Skinner W, Villa A, Liberman H, Younis G, de Silva R, Diaz M, Tami I, Hodgson J, Raveendran G, Goswami N, Arias J, Lovitz L, Carida Ii R, Pottluri S, Prati F, Erglis A, Pop A, McEntegart M, Hudec M, Rangasetty U, Newby D. Identification of patients and plaques vulnerable to future coronary events with near-infrared spectroscopy intravascular ultrasound imaging: a prospective, cohort study. *Lancet* 2019;394:1629-1637.
52. Oemrawsingh RM, Cheng JM, Garcia-Garcia HM, Geuns R-JV, Boer SD, Simsek C, Kardys I, Lenzen MJ, Domburg RV, Regar E, Serruys PW, Akkerhuis KM, Boersma E; ATHEROREMO-NIRS Investigators. Near-infrared spectroscopy predicts cardiovascular outcome in patients with coronary artery disease. *J Am Coll Cardiol* 2014;64:2510-2518.
53. Goldstein JA, Maini B, Dixon SR, Brilakis ES, Grines CL, Rizik DG, Powers ER, Steinberg DH, Shunk KA, Weisz G, Moreno PR, Kini A, Sharma SK, Hendricks MJ, Sum ST, Madden SP, Muller JE, Stone GW, Kern MJ. Detection of lipid-core plaques by intracoronary near-infrared spectroscopy identifies high risk of periprocedural myocardial infarction. *Circ Cardiovasc Interv* 2011;4:429-437.
54. Dixon SR, Grines CL, Munir A, Madder RD, Safian RD, Hanzel GS, Pica MC, Goldstein JA. Analysis of target lesion length before coronary artery stenting using angiography and near-infrared spectroscopy versus angiography alone. *Am J Cardiol* 2012;109:60-66.
55. Horvath M, Hajek P, Muller JE, Honek J, Stechovsky C, Spacek M, Veselka J. First-in-man near-infrared spectroscopy proof of lipidcore embolization during carotid artery stenting. *Arch Med Sci* 2016;12:915-918.